European Journal of Medicinal Chemistry 45 (2010) 1133–1139

Contents lists available at ScienceDirect

European Journal of Medicinal Chemistry

journal homepage: http://www.elsevier.com/locate/ejmech

Original article

Discovery of benzhydrylpiperazine derivatives as CB_1 receptor inverse agonists *via* privileged structure-based approach

Tao Meng [a], Jue Wang [b], Hongli Peng [a,*], Guanghua Fang [a], Min Li [a], Bing Xiong [a], Xin Xie [b,*], Yongliang Zhang [a], Xin Wang [a], Jingkang Shen [a,*]

[a] State Key Laboratory of Drug Research, Shanghai Institute of Materia Medica, Chinese Academy of Sciences, 555 Zuchongzhi Road, Shanghai 201203, PR China
[b] The National Center for Drug Screening, 189 Guoshoujing Road, Shanghai 201203, PR China

ARTICLE INFO

Article history:
Received 23 October 2009
Received in revised form
2 December 2009
Accepted 4 December 2009
Available online 16 December 2009

Keywords:
Benzhydrylpiperazine
Privileged structure
Cannabinoid receptor 1(CB_1)
Anti-obesity

ABSTRACT

The present study describes the identification *via* privileged structure-based approach of the benzhydrylpiperazine moiety as a potential scaffold to develop novel CB_1 receptor modulators. Efficient structural optimization of the initial four hit compounds led to a high quality lead series, represented by compound **6c**. Compound **6c** is a highly potent and selective CB_1 receptor inverse agonist that is able to reduce body weight in diet-induced obese Sprague–Dawley rats. The preparation of privileged structure-based library, the progression from hit to lead, the structure–activity relationships in the lead series and *in vitro* and *in vivo* activity of compound **6c** are discussed.

1. Introduction

The excess consumption of fat-enriched food and sedentary lifestyle result in obesity, which is currently a worldwide health problem [1,2]. In order to discover novel anti-obesity therapeutics, numerous potential drug targets have been studied. Among those, the endocannabinoid system is of particular interest because it plays an important role in the regulation of body energy balance [3]. Cannabinoids and endocannabinoids function *via* two G-protein-coupled receptors (GPCRs) known as CB_1 and CB_2 receptors. CB_1 receptor is mainly expressed in the central nervous system where it controls motivation for appetitive stimuli, including food and drugs. Currently, CB_1 antagonists and inverse agonists are evaluated for obesity, metabolic disorders, smoking cessation, and alcohol abuse [4–6].

Rimonabant (SR141716A), a potent and selective CB_1 receptor inverse agonist, shows promising weight-reducing effect in both animal models and patients. It was launched by Sanofi-Aventis in Europe for the treatment of obesity and associated metabolic disorders [7], but recently withdrawn from the market due to its psychiatric adverse effects (depression and anxiety) [8]. Several other CB_1 receptor inverse agonists including taranabant (MK-0364) and otenabant (CP-945598) were also suspended in late-stage clinical development [9,10]. So far, the mechanisms through which CB_1 receptor blockade increase depression and anxiety remain unclear. It has been noted that CB_1 antagonists are potential usefulness in the treatment of obesity and associated metabolic diseases as well as in other therapeutical areas [9]. Hence, developing novel CB_1 receptor antagonists with unique structure and pharmacological properties may provide an option to overcome the safety problems associated with current CB_1 antagonists and optimize the therapeutic benefits of CB_1 receptor antagonists.

Scaffold hopping and bioisosteric approaches have been previously applied in discovery of CB_1 receptor antagonists [11–13]. However, the majority of the reported CB_1 receptor antagonists and inverse agonists can be described in terms of a general pharmacophore model [12]. The privileged structure concept has also been used extensively to design libraries that possess a high probability of producing lead compounds against a variety of targets, especially for GPCRs [14–16]. A privileged structure is a molecular scaffold that is able to provide potent and selective ligands for a range of different biological targets through modification of functional groups, and usually exhibits good drug-like properties that lead to more drug-like compound libraries and leads [14,16].

Given the success of privileged structures in medicinal chemistry, we envisioned that a similar application of this concept could rapidly identify novel CB_1 antagonists. Herein, we report the

* Corresponding authors. Tel.: +86 21 50806600 5407; fax: +86 21 50807088.
E-mail addresses: penghl@mail.shcnc.ac.cn (H. Peng), xxie@mail.shcnc.ac.cn (X. Xie), jkshen@mail.shcnc.ac.cn (J. Shen).

0223-5234/$ – see front matter © 2009 Elsevier Masson SAS. All rights reserved.
doi:10.1016/j.ejmech.2009.12.018

identification of the benzhydrylpiperazine moiety as a potential scaffold to develop novel CB_1 receptor modulators utilizing privileged structure-based approach.

2. Results and discussion

2.1. Privileged structure-based library construction and CB_1 hits identification

The preparation of privileged structure-based library and general screening data of this library are outlined in Fig. 1. Six molecular frameworks, including diphenylmethane, 2-aminothiazole, benzimidazole, piperazine, 4-aminopiperidine, and 1,2-diphenyl-substituted five-membered heterocyclic fragments were selected as privileged structure subunits as these structures are widely present in many GPCR ligands [14–16]. Furthermore, phenyl-substituted bicyclic framework have been utilized frequently in medicinal chemistry, and is commonly observed as core elements of privileged substructures [17]. We then designed and synthesized a privileged structure-based library of bicyclic compounds, including substituted benzhydryloxyalkyl guanidines (array 1), 1-phenylbenzimidazoles (array 2), 4,5-diphenyl-2-aminothiazoles (array 3), *N*-benzhydrylpiperidin-4-amines (array 4), diphenylpiperazines (array 5), and 1-phenyl-1,2,3,4-tetrahydroisoquinolines (array 6), by using the selected privileged subunits.

This library was evaluated by screening against several GPCRs, including the human CB_1 (hCB_1) and CB_2 (hCB_2) receptors, melanocortin receptor 4 (MC4R), chemokine receptor 5 (CCR5), and neuromedin U receptor 1/2 (NMUR1/2), utilizing radioligand binding or functional Ca^{2+} flux assays. The *in vitro* activities are summarized in Fig. 1 and Table 1. Of the six arrays, only array 5 was selective, exhibiting high binding affinity for hCB_1 (K_i values ranging from 50 to 250 nM). In addition, array 3 was selective to CCR5 ($K_i < 6.5$ μM), while array 1 showed activity at both of MC4R ($K_i < 10$ μM) and NMUR1/2 ($K_i < 10$ μM). Remarkably, high hit rates of ~6% can be observed with this privileged structure library of 230 compounds, indicating the successful use of the GPCR-based privileged structure approach for hit finding.

2.2. Structure–activity relationships (SAR) of benzhydrylpiperazine derivatives at hCB_1 receptor

As shown in Table 1, four CB_1 hits identified *via* privileged structure-based approach share the same benzhydrylpiperazine core structure that occurs in well-known class of antihistamine drugs [18], and is a novel scaffold for CB_1 modulators. Therefore, this class of compounds was explored for further SAR studies.

Synthesis of the benzhydryl-1,4-diazepanes **1**(**a**–**d**) is illustrated in Scheme 1. The intermediate 1-benzhydryl-1,4-diazepane was synthesized by condensation of homopiperazine with diphenylmethyl chloride, followed by reaction with the corresponding acyl chlorides, isocyanates and thioisocyanates to afford the desired amide **1a**, ureas **1**(**b**–**c**), and thiourea **1d**.

The benzhydrylpiperazine derivatives **4**(**a**–**g**), **5**(**a**–**i**), and **6**(**a**–**h**) were prepared according to Scheme 2. The key intermediates **2**(**a**–**n**) were synthesized by Grignard reaction of substituted phenylmagnesium bromide, followed by addition of the substituted benzaldehyde in THF. Treatment of **2**(**a**–**n**) with thionyl chloride followed by refluxing with piperazine in acetonitrile afforded the intermediates **3**(**a**–**n**). The target compounds were obtained by the coupling reaction of intermediate **3**(**a**–**n**) with corresponding acyl chlorides, isocyanates and thioisocyanates.

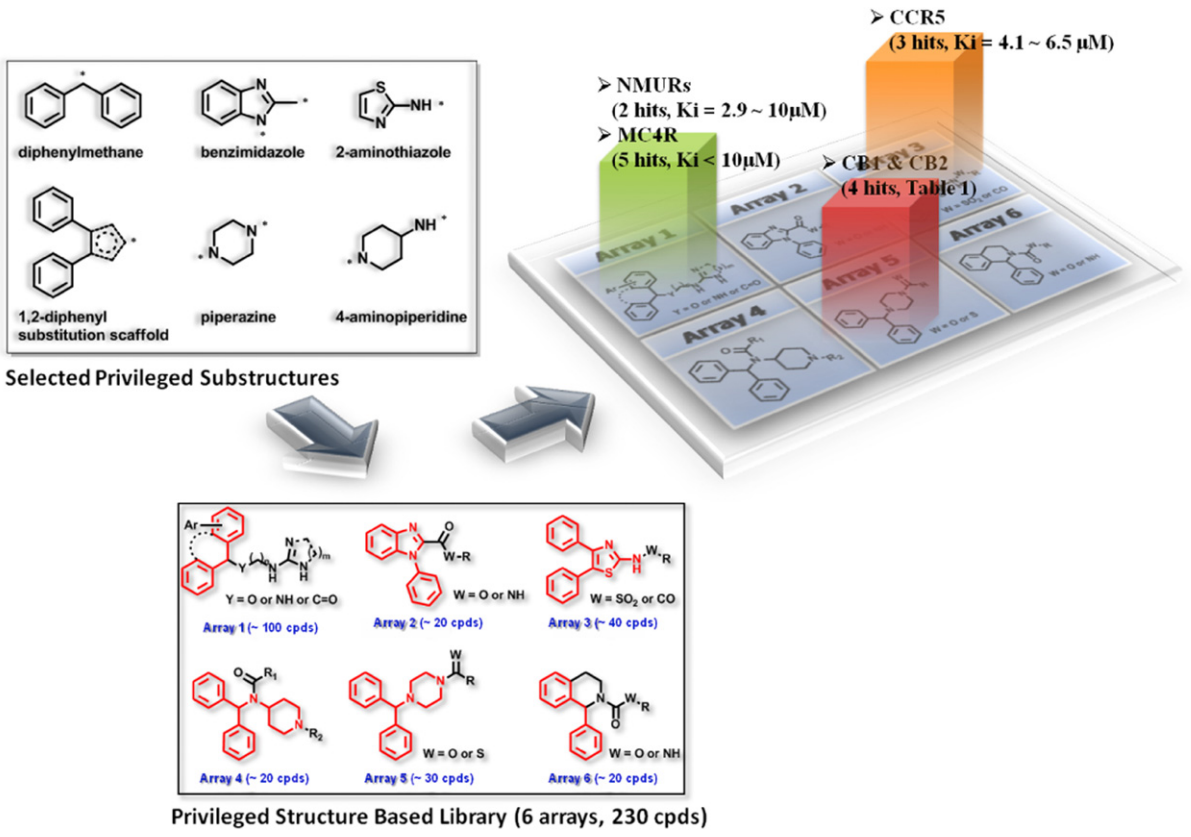

Fig. 1. Design of privileged structure-based library targeting GPCRs and pharmacological screening results.

Table 1
Activity of array **5** from the privileged structure-based library.[a]

Cpd.	R	hCB_1 K_i (nM)	hCB_2 K_i (nM)	hCB_1 Ca^{2+} IC_{50} (nM)
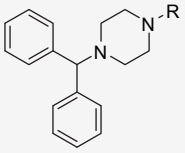				
Rimonabant	–	0.74 ± 0.10	126 ± 12	3.2 ± 0.3
hit-1	Cyclohexylamide	164 ± 16	3050 ± 824	ND
hit-2	Cyclohexylurea	52 ± 13	2407 ± 538	ND
hit-3	*n*-Butylurea	239 ± 95	2833 ± 361	ND
hit-4	Cyclohexylthiourea	106 ± 26	1866 ± 146	ND

[a] K_i and IC_{50} (mean ± SEM) ($n \geq 3$ independent experiments) were calculated from dose-response curves. hCB_1: human CB_1 receptor. hCB_2: human CB_2 receptor. ND: not detected. Rimonabant: CB_1 reference compound.

All the target compounds were evaluated *in vitro* at the hCB_1 and hCB_2 receptors, stably expressed into Chinese Hamster Ovary (CHO) cells, utilizing radioligand binding studies. CB_1 receptor antagonism was measured using a CP-55940 (an agonist of the CBRs) induced Ca^{2+} increase functional assay in CHO cells co-expressing hCB_1 receptor and Gα15/16.

The general structure of identified hit compounds was divided into four fragments (A–D shown in Fig. 2), and each fragment was modified for the SAR study separately. We first examined whether enlargement of the piperazine ring (fragment A) would improve hCB_1 activity. Replacement of piperazine with homopiperazine led to a complete loss of binding affinity (K_i > 10,000 nM) for both hCB_1 and hCB_2, indicating that piperazine is essential to the biological activity.

The SAR from the hit compounds demonstrated that the cyclohexylurea in fragment C (Table 1, hit 2) correlated with relative higher binding affinity and selectivity for hCB_1. Keeping fragment C as the cyclohexylurea and fragment D unaltered, various halogens

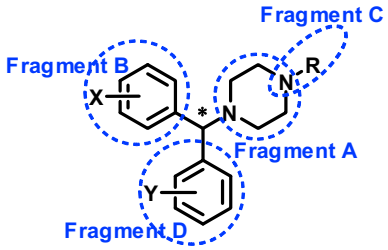

Fig. 2. Four fragments of the benzhydrylpiperazine core structure.

at different positions of the phenyl ring in fragment B were examined. As shown in Table 2, the 2,4-dichlorophenyl(**4a**), 2,5-dichlorophenyl(**4c**), 2,6-dichlorophenyl(**4d**), 2-fluoro-4-bromophenyl(**4e**), 2-chloro-4-fluorophenyl(**4f**), and 2-fluoro-4-chlorophenyl(**4g**) significantly improved the hCB_1 affinity as well as selectivity over hCB_2, except the 3,4-dichloro substitution (**4b**), indicating that *ortho*-substitution in fragment B is necessary for high affinity for hCB_1. Functional Ca^{2+} assay revealed that this series of compounds had inhibitory effects on CP-55940-induced Ca^{2+} increase. Among these hCB_1 antagonists, the 2,4-dichlorophenyl moiety (**4a**) showed the best hCB_1 binding affinity as well as antagonistic activity.

Having identified 2,4-dichloro as the optimal substitution of the phenyl ring in fragment B, various acyl (amide, urea, thiourea) wherein substituent was a 4–10 atom aliphatic ring or chain were examined for the SAR of fragment C. As shown in Table 3, transformation of urea of **4a** to amide to give **5c** or replacement of cyclohexyl ring of **4a** with piperidinyl to give **5h** had a small or no effect on binding affinity, but resulted in an increase in selectivity for hCB_1. On the other hand, a great loss in hCB_1 activity was observed when the cyclohexyl ring of **4a** was replaced by the *n*-butyl (**5g**), indicating the importance of the aliphatic ring structure. Similarly, cyclohexylthiourea (**5i**) enhanced binding affinity and selectivity for the hCB_1 receptor.

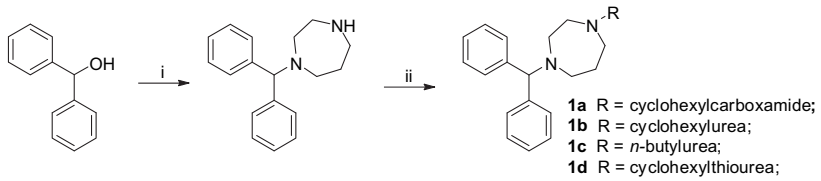

Scheme 1. Reagents and conditions: (i) $SOCl_2$, CH_2Cl_2, rt; homopiperazine, CH_3CN, reflux; (iii) for compound **1a**: cyclohexanecarbonyl chloride, Et_3N, CH_2Cl_2, rt; for compound **1b**–**c**: isocyanates, CH_2Cl_2, rt; for compound **1d**: cyclohexyl isothiocyanate, CH_2Cl_2, rt.

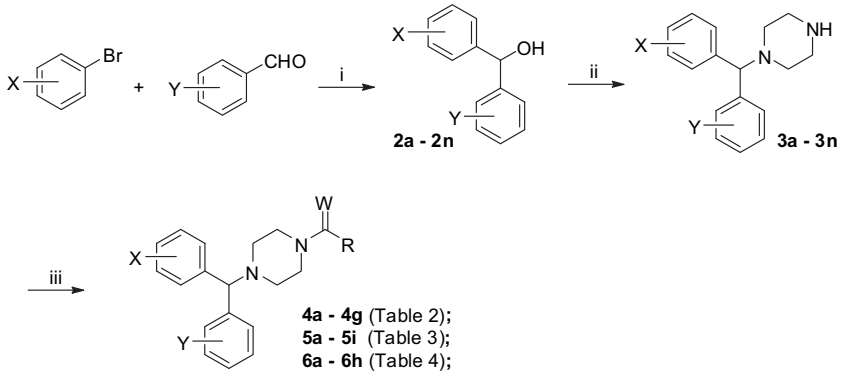

Scheme 2. Reagents and conditions: (i) Mg/THF, rt then reflux; (ii) $SOCl_2$, CH_2Cl_2, rt; piperazine, CH_3CN, reflux; (iii) isocyanates, CH_2Cl_2, rt, or acyl chlorides, Et_3N, CH_2Cl_2, rt, or thioisocyanates, CH_2Cl_2, rt.

Table 2
SAR of Fragment B Modification at hCB_1 receptor.[a]

Cpd.	X	hCB_1 K_i (nM)	hCB_2 K_i (nM)	hCB_1 Ca^{2+} IC_{50} (nM)
	Fragment B			
4a	2,4-diCl	1.6 ± 0.2	432 ± 118	9.2 ± 1.6
4b	3,4-diCl	60 ± 17	356 ± 174	462 ± 97
4c	2,5-diCl	5.9 ± 1.7	899 ± 292	43 ± 18
4d	2,6-diCl	2.2 ± 0.3	831 ± 169	55 ± 37
4e	2-F-4-Br	1.8 ± 0.5	322 ± 89	87 ± 11
4f	2-Cl-4-F	8.1 ± 1.5	1300 ± 309	68 ± 26
4g	2-F-4-Cl	3.1 ± 1.4	526 ± 432	124 ± 52

[a] K_i and IC_{50} (mean ± SEM) ($n \geq 3$ independent experiments) were calculated from dose-response curves. hCB_1: human CB_1 receptor. hCB_2: human CB_2 receptor.

Following the above results, we decided to conduct the SAR studies of fragment D on structures with 2,4-dichloro substitution as fragment B, and cyclohexylurea and 1-(piperidin-1-yl)urea as fragment C, respectively. The cyclohexylthiourea (**5i**) was excluded due to the toxicity of thiourea [19]. As shown in Table 4, different substituents at the *meta*-/*para*-position of the phenyl ring in fragment D did not significantly influence binding affinity, but caused a decrease in selectivity for hCB_1. Only cyclohexylurea derivatives with *para*-methyl substitution (**6c**) showed high potency ($K_i = 0.15$ nM) and selectivity (>2000) for hCB_1.

The inverse agonist property of compound **6c** was studied using a functional cAMP assay in CHO cell expressing the hCB_1 receptor. Because CB_1 receptor is a Gi/o-coupled receptor, activation of hCB_1 by CP55940 led to a dose-dependent inhibition of forskolin-stimulated cAMP increase, whereas the inverse agonist, rimonabant, further facilitated cAMP production. As shown in Fig. 3A, compound **6c** ($EC_{50} = 0.87$ nM) displayed a similar cAMP stimulation pattern as rimonabant ($EC_{50} = 0.11$ nM) under the same assay conditions. Thus, compound **6c** appears to be a potent CB_1 inverse agonist.

2.3. In vivo studies

Following a single oral administration of 10 mg/kg in Sprague–Dawley rats, the plasma half-life of compound **6c** is approximately 2.4 h and the plasma-to-brain concentration ratios were 0.5 and about 1.0, respectively at 3 and 12 h postdose (Fig. 3B). The plasma-to-brain concentration ratios of rimonabant (10 mg/kg, p.o.) were 1.6 and near 4.4, respectively at 3 and 12 h postdose (Fig. 3B). Compared with rimonabant, compound **6c** was slowly and lowly brain-penetrant. In diet-induced obesity (DIO) rats, a single dose of

Table 3
SAR of Fragment C Modification at hCB_1 receptor.[a]

Cpd.	R	hCB_1 K_i (nM)	hCB_2 K_i (nM)	hCB_1 Ca^{2+} IC_{50} (nM)
	Fragment C			
5a	Cyclobutylamide	291 ± 35	2116 ± 273	> 10,000
5b	Cyclopentylamide	732 ± 186	4885 ± 1911	403 ± 95
5c	Cyclohexylamide	5.8 ± 1.5	2928 ± 1104	9.3 ± 8.5
5d	Adamantylamide	5.9 ± 1.7	25 ± 16	288 ± 256
5e	Piperidylamide	56 ± 23	987 ± 206	>10,000
5f	4-Morpholylamide	111 ± 59	618 ± 251	>10,000
5g	*n*-Butylurea	103 ± 50	918 ± 353	173 ± 30
5h	1-(Piperidin-1-yl)urea	1.2 ± 0.2	1043 ± 495	4.7 ± 2.5
5i	Cyclohexylthiourea	0.20 ± 0.08	673 ± 94	18 ± 6

[a] K_i and IC_{50} (mean ± SEM) ($n \geq 3$ independent experiments) were calculated from dose-response curves. hCB_1: human CB_1 receptor. hCB_2: human CB_2 receptor.

Table 4
SAR of Fragment D Modification at hCB_1 receptor.[a]

Cpd	Y	R	hCB_1 K_i (nM)	hCB_2 K_i (nM)	hCB_1 Ca^{2+} IC_{50} (nM)
		Fragment D			
6a	3-Cl	Cyclohexylurea	2.3 ± 0.4	407 ± 271	161 ± 75
6b	4-Cl	Cyclohexylurea	0.23 ± 0.06	26 ± 2	19 ± 6
6c	4-CH_3	Cyclohexylurea	0.15 ± 0.04	329 ± 71	2.7 ± 0.5
6d	4-CH_3	1-(Piperidin-1-yl)urea	3.0 ± 1.2	317 ± 67	15 ± 2
6e	4-OCH_3	Cyclohexylurea	2.6 ± 1.4	290 ± 197	82 ± 13
6f	4-OPh	Cyclohexylurea	1.1 ± 0.4	52 ± 10	34 ± 3
6g	4-CF_3	Cyclohexylurea	1.2 ± 0.3	274 ± 34	57 ± 41
6h	4-F	Cyclohexylurea	2.5 ± 1.1	159 ± 34	8.1 ± 1.4

[a] K_i and IC_{50} (mean ± SEM) ($n \geq 3$ independent experiments) were calculated from dose-response curves. hCB_1: human CB_1 receptor. hCB_2: human CB_2 receptor.

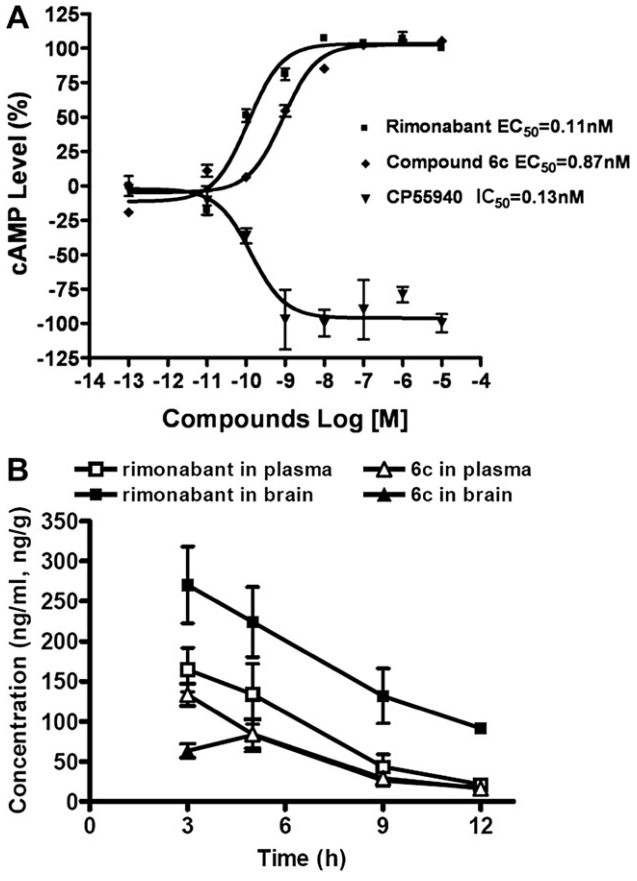

Fig. 3. (A) Whole-cell cAMP assay using CHO cells expressing human CB_1 receptor. (B) Plasma (ng/mL) and brain (ng/g) concentration–time courses of compound **6c** and rimonabant following a single oral administration of 10 mg/kg in Sprague–Dawley rats. Data represent mean ± SE ($n = 5$ rats/group).

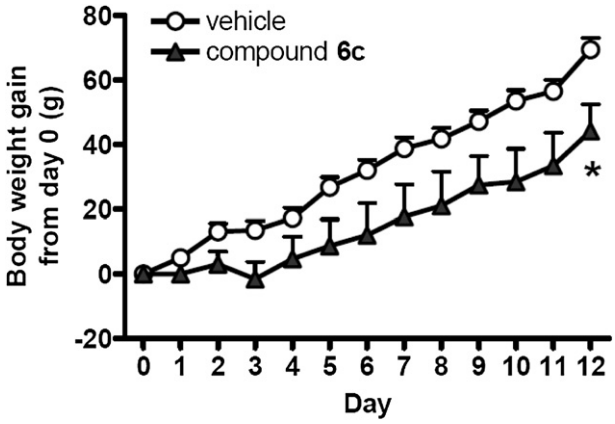

Fig. 4. Chronic effects of compound **6c** in DIO rats. A significant reduction in body weight gain was observed on days 12 at 10 mg/kg of compound **6c**. *$P < 0.05$ vs vehicle. Data represent mean ± SE ($n = 11$–12 rats/group).

compound **6c** at 10 mg/kg (p.o.) suppressed 3 h and overnight (18 h) food intake by 39% and 22%, respectively. Furthermore, the *in vivo* efficacy of compound **6c** in body weight reduction was assessed with the DIO rat model. Chronic application of compound **6c** (10 mg/kg, p.o.) once daily for 12 days led to a slower progression of body weight and a significant reduction in the final body weight gain on day 12 from starting weight ($p < 0.05$, Fig. 4).

3. Conclusion

In this study, we described the identification *via* privileged structure-based approach of benzhydrylpiperazine moiety as a potential scaffold to develop novel CB_1 receptor modulators. Efficient structural optimization of the initial hit compounds led to the discovery of high quality lead series, represented by compound **6c**. Compound **6c** is a highly potent and selective CB_1 inverse agonist that is able to reduce body weight gain in a DIO rat model. A study by Song et al. [20] has depicted similar derivatives that revealed very low CB_1 binding activities, however, there were no cellular function and *in vivo* information of such structures reported in this study.

4. Experiment procedure

4.1. Synthesis

All non-aqueous reactions were performed in dried glassware under an atmosphere of Ar, unless otherwise specified. THF was freshly distilled from sodium/benzophenone under Ar. All solvents are of the highest available purity unless otherwise indicated. Melting points were determined in open capillary tubes on an electrothermal melting point apparatus. ^{1}H and ^{13}C NMR spectra were recorded on Varian Mercury-400 spectrometer. Chemical shifts are reported in ppm from TMS with the solvent resonance as the internal standard. The following abbreviations were used to explain the multiplicities: s = singlet, d = doublet, t = triplet, q = quartet, dd = doublet of doublets, m = multiplet, br = broad. The LC-MS was carried out on Thermo Finnigan LCQDECAXP. Low-resolution mass spectra were performed on Finnigan MAT 95 and Finnigan LCQ Deca spectrometers and high resolution mass spectra were measured on Finnigan MAT 95 and MicroMass Q-Tof ultima™ mass spectrometers. General synthetic procedures used for the preparation of the selected target compounds **4a**, **5c**, **5g–i** and **6b–d** are described as follows.

4.1.1. General method for synthesis of 1-[(2,4-dichlorophenyl)(phenyl)methyl] piperazine (**3a**)

To a solution of 2,4-dichlorobenzaldehyde (10.0 g, 0.57 mol) in anhydrous THF (100 mL) phenylmagnesium bromide (80 mL, freshly prepared 0.9 M solution in THF) was added dropwise at room temperature. After 1 h of stirring the reaction mixture was treated with saturated NH_4Cl aqueous solution (10 mL) and diethyl ether (300 mL) and organic phase was washed successively with brine and dried over anhydrous Na_2SO_4. After evaporation of the solvent under vacuum the crude product (2,4-dichlorophenyl)(phenyl)methanol (**2a**, 12.7 g, 88%) was obtained and used in following reactions without further purification. ^{1}H NMR (400 MHz, $CDCl_3$) δ 7.59(d, $J = 8.4$ Hz, 1H), 7.26–7.38(m, 9H), 6.16(d, $J = 3.7$ Hz, 1H).

Benzhydrol (**2a**) was dissolve in CH_2Cl_2 (70 mL). After addition of $SOCl_2$ (5 mL, 0.69 mol) the reaction mixture was stirred at 40 °C for 3 h. The solvent was evaporated under vacuum and the residue was dissolved in MeCN (80 mL). Then, piperazine (24.6 g, 0.29 mol) was added and the mixture was refluxed for 12 h. The solvent was removed under vacuum and the residue was dissolved in ethyl acetate (250 mL) and washed with water (100 mL) followed by 1 N HCl (100 mL). The acid phase was washed with ethyl acetate (3 × 60 mL). The ethyl acetate layer was discarded and the remaining water layer was neutralized with 3 N NaOH aqueous solution (40 mL) to pH > 10. The aqueous solution was extracted with CH_2Cl_2 (3 × 80 mL). The combined CH_2Cl_2 was washed successively with brine, dried over Na_2SO_4 and evaporated under vacuum to provide the title compound **3a** as a yellow oil (12.5 g, 78%). ^{1}H NMR (400 MHz, $CDCl_3$) δ 7.73(dd, $J = 12.5$, 8.4 Hz, 1H), 7.35–7.39(m, 2H), 7.17–7.31(m, 5H), 4.72(s, 1H), 3.09–3.12(m, 2H), 2.59(br s, 2H), 2.48(br s, 2H), 2.37(br s, 2H); ESI: *m*/*z* (relative intensity) 320.9(M + 1, 100%), 235.0.

4.1.2. 1-[(4-Chlorophenyl)(2,4-dichlorophenyl)methyl]piperazine (**3i**)

The procedure described for the synthesis of **3a** was applied to synthesize the title compound **3i** as a yellow oil in 62% total yield. ^{1}H NMR (400 MHz, $CDCl_3$) δ 7.71(d, $J = 8.4$ Hz, 1H), 7.23–7.36(m, 6H), 4.71(s, 1H), 2.85–2.88(m, 4H), 2.32–2.47(m, 4H). ESI: *m*/*z* (relative intensity) 354.9(M + 1, 100%), 269.0.

4.1.3. 1-[(2,4-Dichlorophenyl)(p-tolyl)methyl]piperazine (**3j**)

The procedure described for the synthesis of **3a** was applied to synthesize the title compound **3j** as a yellow oil in 64% total yield. ^{1}H NMR (400 MHz, $CDCl_3$) δ 7.73(dd, $J = 13.5$, 8.4 Hz, 1H), 7.20–7.30(m, 4H), 7.05–7.10(m, 2H), 4.69(s, 1H), 3.14–3.17(m, 2H), 2.65(br s, 2H), 2.52(br s, 2H), 2.38(br s, 2H), 2.28(s, 3H). ESI: *m*/*z* (relative intensity) 334.9(M + 1, 100%), 249.0.

4.1.4. N-Cyclohexyl-4-[(2,4-dichlorophenyl)(phenyl)methyl]-piperazine-1-carboxamide (**4a**)

To a solution of compound **3a** (0.20 g, 0.62 mmol) in CH_2Cl_2 (5 mL) cyclohexyl isocyanate (0.78 g, 0.62 mmol) was added. The reaction mixture was subsequently stirred at room temperature overnight, and evaporated under vacuum to get the crude product. The residue was further purified by flash column chromatography, petroleum ether:EtOAc (10:1 → 2:1) as an eluent to afford the title compound **4a** as a white solid (0.22 g, 79%), mp 165–168 °C. ^{1}H NMR (400 MHz, $CDCl_3$) δ 7.75(d, $J = 8.5$ Hz, 1H), 7.38–7.41(m, 2H), 7.18–7.30(m, 5H), 4.75(s, 1H), 4.21(d, $J = 7.6$ Hz, 1H, NH), 3.63(m, 1H), 3.31(m, 4H), 2.37(m, 4H), 1.93(dd, $J = 12.5$, 3.1 Hz, 2H), 1.57–1.72(m, 3H), 1.32–1.39(m, 2H), 1.04–1.16(m, 3H). ^{13}C NMR ($CDCl_3$) δ 157.04, 140.13, 138.49, 134.35, 132.96, 129.68, 129.45, 128.59 × 2, 128.31 × 2, 127.54 × 2, 69.83, 51.39(2 × CH_2), 49.32, 43.80(2 × CH_2), 33.93(2 × CH_2), 25.62(CH_2), 25.01(2 × CH_2). HRMS(EI) *m*/*z* calcd for $C_{24}H_{29}Cl_2N_3O$, 445.1688; found, 445.1683.

4.1.5. 1-(Cyclohexylcarbonyl)-4-[(2,4-dichlorophenyl)(phenyl)methyl]piperazine (**5c**)

To a solution of compound **3a** (0.20 g, 0.62 mmol) and triethylamine (0.17 mL, 1.3 mmol) in 5 mL dichloromethane, cyclohexanecarbonyl chloride (84 μL, 0.62 mmol) was added with stirring at 0 °C. The reaction mixture was then stirred at room temperature overnight and poured into water. The mixture was extracted with CH_2Cl_2 (2 × 20 mL). The combined CH_2Cl_2 was washed with water and brine, dried over Na_2SO_4, and evaporated under vacuum. The residue was further purified by flash column chromatography, petroleum ether:EtOAc (10:1 → 3:1) as an eluent to afford the title compound **5c** as a white solid (0.23 g, 87%), mp 125–128 °C. ^{1}H NMR (400 MHz, $CDCl_3$) δ 7.77(d, J = 8.1 Hz, 1H), 7.22–7.41(m, 7H), 4.75(s, 1H), 3.59(m, 2H), 3.48(m, 2H), 2.38(m, 5H), 1.79(m, 2H), 1.67–1.71(m, 4H), 1.48–1.52(m, 2H), 1.22(m, 2H). ^{13}C NMR ($CDCl_3$) δ 174.44, 140.01, 138.37, 134.35, 133.02, 129.63, 129.48, 128.63 × 2, 128.29 × 2, 127.57 × 2, 69.85, 52.23(CH_2), 51.65(CH_2), 45.40(CH_2), 41.53(CH_2), 40.36, 29.34(CH_2), 29.29(CH_2), 25.81(3 × CH_2). HRMS(EI) m/z calcd for $C_{24}H_{28}Cl_2N_2O$, 430.1579; found, 430.1581.

4.1.6. N-Butyl-4-[(2,4-dichlorophenyl)(phenyl)methyl]piperazine-1-carboxamide (**5g**)

The procedure described for the synthesis of **4a** was applied to **3a** and *n*-butylisocyanate providing the title compound **5g** as a white solid in 86% yield, mp 125–127 °C. ^{1}H NMR (400 MHz, $CDCl_3$) δ 7.75(d, J = 9.2 Hz, 1H), 7.24–7.41(m, 7H), 4.75(s, 1H), 3.33(m, 4H), 3.18–3.25(m, 2H), 2.37(m, 4H), 1.43–1.52(m, 2H), 1.29–1.37(m, 2H), 0.92(t, J = 7.3 Hz, 3H). ^{13}C NMR ($CDCl_3$) δ 157.78, 140.10, 138.46, 134.33, 132.95, 129.67, 129.44, 128.59 × 2, 128.29 × 2, 127.54 × 2, 69.83, 51.40(2 × CH_2), 43.80(2 × CH_2), 40.58(CH_2), 32.30(CH_2), 20.05(CH_2), 13.80. HRMS(EI) m/z calcd for $C_{22}H_{27}Cl_2N_3O$, 419.1531; found, 419.1533.

4.1.7. 4-[(2,4-Dichlorophenyl)(phenyl)methyl]-N-piperidin-1-ylpiperazine-1-carboxamide (**5h**)

To a solution of 1,1′-carbonyldiimidazole(CDI, 0.18 g, 1.1 mmol) in THF (10 mL) was added a solution of 1-aminopiperidine(0.11 g, 1.1 mmol) in THF (10 mL). The reaction mixture was stirred at ambient temperature for 1.5 h. After addition of a solution of **3a** (0.30 g, 0.93 mmol) in THF (10 mL) the reaction mixture was heated to reflux for 16 h and concentrated. The residue was dissolved in CH_2Cl_2 (100 mL), washed with water and brine, and dried over Na_2SO_4. After evaporation of the solvent under vacuum the residue was further purified by flash column chromatography, petroleum ether:EtOAc (2:1 → 1:2) as an eluent to afford the title compound **5h** as a white solid (0.38 g, 91%), mp 138–140 °C. ^{1}H NMR (400 MHz, $CDCl_3$) δ 7.77(d, J = 8.4 Hz, 1H), 7.38–7.42(m, 2H), 7.19–7.31(m, 5H), 4.97(s, 1H, NH), 4.74(s, 1H), 3.44–3.47(m, 4H), 2.65(br s, 4H), 2.35–2.38(m, 4H), 1.58–1.66(m, 4H), 1.36(m, 2H). ^{13}C NMR ($CDCl_3$) δ 158.28, 140.20, 138.54, 134.34, 132.93, 129.73, 129.43, 128.56 × 2, 128.30 × 2, 127.52, 127.47, 69.93, 57.62(2 × CH_2), 51.66(2 × CH_2), 44.71(2 × CH_2), 25.70(2 × CH_2), 23.21(CH_2); HRMS(EI) m/z calcd for $C_{23}H_{28}Cl_2N_4O$, 446.1640; found, 446.1644.

4.1.8. N-Cyclohexyl-4-[(2,4-dichlorophenyl)(phenyl)methyl]-piperazine-1-carbothioamide (**5i**)

The procedure described for the synthesis of **4a** was applied to **3a** and cyclohexyl isothiocyanate providing the title compound **5i** as a white solid in 92% yield, mp 166–168 °C. ^{1}H NMR (400 MHz, $CDCl_3$) δ 7.76(d, J = 8.5 Hz, 1H), 7.38–7.41(m, 2H), 7.19–7.32(m, 5H), 4.77(s, 1H), 4.33(m, 1H), 3.69–3.83(m, 4H), 2.42–2.45(m, 4H), 2.05–2.11(m, 2H), 1.61–1.73(m, 4H), 1.35–1.46(m, 2H), 1.14(m, 2H). ^{13}C NMR ($CDCl_3$) δ 180.83, 139.84, 138.16, 134.35, 133.10, 129.57, 129.50, 128.64, 128.25 × 2, 127.63 × 2, 127.58, 69.62, 54.14, 51.12(2 × CH_2), 47.15(2 × CH_2), 33.07(2 × CH_2), 25.53(CH_2), 24.84(2 × CH_2). ESI: m/z (relative intensity) 462.0(M + 1, 100%), 235.0; HRMS(EI) m/z calcd for $C_{24}H_{29}Cl_2N_3S$, 461.1459; found, 416.1456.

4.1.9. 4-[(4-Chlorophenyl)(2,4-dichlorophenyl)methyl]-N-cyclohexylpiperazine-1-carboxamide (**6b**)

The procedure described for the synthesis of **4a** was applied to **3i** and cyclohexyl isocyanate providing the title compound **6b** as a white solid in 89% yield, mp 172–175 °C, ^{1}H NMR (400 MHz, $CDCl_3$) δ 7.70(d, J = 8.2 Hz, 1H), 7.27–7.36(m, 6H), 4.73(s, 1H), 4.21(d, J = 7.3 Hz, 1H, NH), 3.63(m, 1H), 3.32(t, J = 5.0 Hz, 4H), 2.36(ddd, J = 20.2, 11.2, 4.4 Hz, 4H), 1.93(dd, J = 12.5, 3.4 Hz, 2H), 1.57–1.72(m, 3H), 1.26–1.43(m, 2H), 1.01–1.18(m, 3H). ^{13}C NMR ($CDCl_3$) δ 156.99, 138.70, 137.96, 134.28, 133.26 × 2, 129.58 × 2, 129.51 × 2, 128.82 × 2, 127.68, 69.14, 51.35(2 × CH_2), 49.35, 43.76(2 × CH_2), 33.93(2 × CH_2), 25.62(CH_2), 25.00(2 × CH_2). HRMS(EI) m/z calcd for $C_{24}H_{28}Cl_3N_3O$, 479.1298; found, 479.1296.

4.1.10. N-Cyclohexyl-4-[(2,4-dichlorophenyl)(p-tolyl)methyl]piperazine-1-carboxamide (**6c**)

The procedure described for the synthesis of **4a** was applied to **3j** and cyclohexyl isocyanate providing the title compound **6c** as a white solid in 90% yield, mp 143–146 °C. ^{1}H NMR (400 MHz, $CDCl_3$) δ 7.76(d, J = 8.4 Hz, 1H), 7.23–7.29(m, 4H), 7.07–7.09(m, 2H), 4.70(s, 1H), 4.21(d, J = 7.7 Hz, 1H, NH), 3.63(m, 1H), 3.29–3.32(m, 4H), 2.35–2.37(m, 4H), 2.29(s, 3H), 1.91–1.95(m, 2H), 1.66–1.71(m, 2H), 1.59–1.62(m, 2H), 1.31–1.38(m, 2H), 1.03–1.14(m, 2H). ^{13}C NMR ($CDCl_3$) δ 157.04, 138.75, 137.22, 137.07, 134.27, 132.83, 129.57, 129.43, 129.27 × 2, 128.22 × 2, 127.50, 69.58, 51.38(2 × CH_2), 49.31, 43.80(2 × CH_2), 33.93(2 × CH_2), 25.63(CH_2), 25.01(2 × CH_2), 21.05. HRMS(EI) m/z calcd for $C_{25}H_{31}Cl_2N_3O$, 459.1844; found, 459.1837.

4.1.11. 4-[(2,4-Dichlorophenyl)(p-tolyl)methyl]-N-piperidin-1-ylpiperazine-1-carboxamide (**6d**)

The procedure described for the synthesis of **5h** was applied to **3j** and 1-aminopiperidine providing the title compound **6d** as a white solid in 89% yield, mp 167–168 °C. ^{1}H NMR (400 MHz, $CDCl_3$) δ 7.78(d, J = 8.4 Hz, 1H), 7.23–7.30(m, 4H), 7.08–7.10(m, 2H), 4.91(s, 1H, NH), 4.70(s, 1H), 3.43–3.47(m, 4H), 2.64(m, 4H), 2.34–2.37(m, 4H), 2.29(s, 3H), 1.58–1.66(m, 4H), 1.36(m, 2H). ^{13}C NMR ($CDCl_3$) δ 158.29, 138.80, 137.18, 137.14, 134.27, 132.81, 129.62, 129.40, 129.26 × 2, 128.22 × 2, 127.49, 69.69, 57.60(2 × CH_2), 51.66(2 × CH_2), 44.71(2 × CH_2), 25.71(2 × CH_2), 23.22(CH_2), 21.02. HRMS(EI) m/z calcd for $C_{24}H_{30}Cl_2N_4O$, 460.1797; found, 460.1791.

4.2. Biology

4.2.1. Cell culture and preparation of stably transfected CHO cells

Chinese hamster ovarian (CHO) cells were stably transfected with the plasmid encoding hCB_1 or hCB_2 receptors cloned by our laboratory. The recombinant CHO-hCB_1/hCB_2 cells were grown in F12 nutrient medium with 10% FBS, 100 mg/L penicillin, 100 mg/L streptomycin, and 1 mg/mL G418. After confluence, cells were trypsinized and collected by centrifugation at 800 rpm for 5 min, planted onto 96-well plates at the density of 20,000 cells per well and incubated at 37 °C in a humidified atmosphere of 5% CO_2 overnight. CHO cells co-transfected with hCB_1 receptors and Gα15/16 (CHO-hCB_1-Gα15/16) were plated onto 96-well plates at a density of 30,000 cells/100 μL/well and cultured in same conditions.

4.2.2. Whole-cell binding assay

The assay was performed using recombinant CHO-hCB_1/hCB_2 cells prepared as previously described. In briefly, cells were starved in serum-free F12 medium for 3 h and pretreated with different concentrations of rimonabant or test compounds for 10 min before the addition of [^{3}H]-CP-55940. After 3 h incubation at 37 °C, cells

were washed 5 times with prewarmed phosphate-buffered saline (PBS) and lysed by PBS with 1% SDS. The lysed pellets were transferred into 96-well isoplate (PerkinElmer, Waltham, MA, USA) and bound radioligand was measured with 1450 microbeta liquid scintillation luminescence counter (PerkinElmer, Waltham, MA, USA). Assays were performed in triplicate. IC_{50} values were analyzed by nonlinear regression analysis performed using the GraphPad Prism 4.0 software (GraphPad Software, San Diego). The K_i values were calculated by the Cheng–Prusoff equation: $K_i = IC_{50}/(1 + L/Kd)$.

4.2.3. Calcium current assay

CHO-hCB_1-Gα15/16 cells were loaded with 2 μM fluo-4 AM in Hanks balanced salt solution (HBSS, containing 5.4 mM KCl, 0.3 mM Na_2HPO_4, 0.4 mM KH_2PO_4, 4.2 mM $NaHCO_3$, 1.3 mM $CaCl_2$, 0.5 mM $MgCl_2$, 0.6 mM $MgSO_4$, 137 mM NaCl, 5.6 mM D-glucose and 250 μM sulfinpyrazone, pH 7.4) at 37 °C for 50 min. After removing the loading buffer, cells were washed with HBSS and incubated with 50 μL HBSS containing various concentrations of test compounds or DMSO (negative control, final concentration 1%). After 10 min incubation at room temperature, 25 μL CP55940 were dispensed into the well by FlexStation II micro-plate reader (Molecular Devices, Sunnyvale, CA, USA), and intracellular calcium change was recorded with an excitation wavelength of 485 nm and emission wavelength of 525 nm. Assays were performed in triplicate.

4.2.4. Intracellular cAMP assay

CHO-hCB_1 cells were harvested with 0.04% EDTA (trypsin free) and diluted to the density of 1×10^6 cells/mL with Stimulation Buffer(1× HBSS, 5 mM HEPES, 0.1% BSA, 0.5 mM IBMX, pH = 7.4). Cells were incubated with the Alexa Fluor 647-anti cAMP antibody (LANCE™ cAMP 384 kit, PerkinElmer, Waltham, MA, USA), forskolin, and various concentration of test compounds or agonist CP55940. After 60 min incubation at room temperature, a detection mix (Eu-W8044 labeled streptavidin 22.2 μM, Biotin-cAMP 4.4 μM, LANCE™ cAMP 384 kit) was added and maintained for 60 min. The mixture was transferred into 384 well assay plate (Corning) and intracellular cAMP levels were measured with Wallac Envision 2101 Multilabel Reader. When adenylyl cyclase is activated by forskolin, activation of Gi by CB1R in the presence of agonist (such as CP55940) will lead to an inhibition of the forskolin-stimulated cAMP increase, and inverse agonist will lead to a further increase. The maximal CP55940-mediated inhibition of forskolin-stimulated cAMP increase is defined as 100% negative efficacy, and the activity of all other compounds is relative to the efficacy of CP55940. Positive efficacy indicates inverse agonist property of test compounds.

4.2.5. In vivo studies

In vivo pharmacological studies in diet-induced obese (DIO) rats were carried out using male Sprague–Dawley rats (Shanghai SLAC Laboratory Animals Co., Shanghai, China). All animal care and experimental procedures carried out in accordance with guidelines of the Laboratory Animal Science Center at Shanghai Institute of Materia Medica. Rats were maintained in a 12 h/12 h light–dark cycle with free access to food and water in group housing conditions in a temperature controlled environment (25 °C). To induce obesity, rats were fed a high fat diet (HFD) containing 1% cholesterol, 0.4% sodium cholate, 32% saturated fat (lard), and 18% casein, with equal quantities of fiber and minerals as in the rat regular diet (Shanghai SLAC Laboratory Animals Co., Shanghai, China) from weaning. The HFD supplied 60% of calories as fat and 20% of calories as carbohydrate comprised of cornstarch and sucrose. Food intake (FI) and body weight (BW) were measured weekly. DIO rats were used at 12–16 weeks of age and conditioned to oral gavage of water for 5 days before experiments.

For inhibition of feeding experiments, DIO rats were randomized into groups ($n = 14$ rats/group) for compounds and vehicle dosing and caged individually in plastic cages. Compound was administered orally to DIO rats 1 h before the start of the dark cycle (4:00 PM) at 10 mg/kg. Vehicle was 0.5% carboxymethyl cellulose in water, and dosing volume was 2 mL/kg. Preweighed pelleted food was provided in food cups that were reweighed at 3 and overnight (18 h) postdose for cumulative food consumed.

For 12-day BW assay, DIO rats ($n = 11$–12 rats/group) were caged individually in plastic cages and dosed orally with vehicle or compound (10 mg/kg) for 12 days. Rats were dosed 1 h before the dark cycle. FI and BW were measured daily. Statistical analysis was performed for the FI and BW data using Student's *t*-test.

4.2.6. Pharmacokinetic assays

Male Sprague–Dawley rats were dosed orally at 10 mg/kg after overnight fasting for pharmacokinetic (PK) evaluations. The blood samples were collected at various time points into lithium heparin tubes and centrifuged. The plasma samples were kept at −20 °C until analysis. For brain penetration study, rats were administered orally at 10 mg/kg and sacrificed at 3, 5, 9 and 12 h postdose, respectively. The whole brains and the blood samples were collected and stored at −20 °C. The plasma samples were extracted by protein precipitation and analyzed by LC/MS/MS. The whole rat brain was homogenized, and was extracted by protein precipitation prior to LC/MS/MS analysis.

Acknowledgment

This work was supported by 863 Program (the National High Technology Research and Development Program of China, No. 2007AA02Z308), by National Science & Technology Major Project "Key New Drug Creation and Manufacturing Program", China (No. 2009ZX09501-010), and grants from the National Natural Science Foundation of China (30672467, 30873162 and 30623008) and Shanghai Commission of Science and Technology (08JC1407701).

Appendix. Supplementary information

Supplementary data associated with this article can be found in the on-line version, at doi:10.1016/j.ejmech.2009.12.018.

References

[1] C. Li, E.S. Ford, A.H. Mokdad, S. Cook, Pediatrics 118 (2006) 1390–1398.
[2] A.H. Mokdad, E.S. Ford, B.A. Bowman, W.H. Dietz, F. Vinicor, V.S. Bales, J.S. Marks, J. Am. Med. Assoc. 289 (2003) 76–79.
[3] S.C. Woods, Am. J. Med. 120 (2007) 19–25.
[4] G. Colombo, A. Orru, P. Lai, C. Cabras, P. Maccioni, M. Rubio, G.L. Gessa, M.A. Carai, Mol. Neurobiol. 36 (2007) 102–112.
[5] J.H. Lange, C.G. Kruse, Chem. Rec. 8 (2008) 156–168.
[6] I. Svizenska, P. Dubovy, A. Sulcova, Pharmacol. Biochem. Behav. 90 (2008) 501–511.
[7] S. Xie, M.A. Furjanic, J.J. Ferrara, N.R. McAndrew, E.L. Ardino, A. Ngondara, Y. Bernstein, K.J. Thomas, E. Kim, J.M. Walker, S. Nagar, S.J. Ward, R.B. Raffa, J. Clin. Pharm. Ther. 32 (2007) 209–231.
[8] R. Christensen, P.K. Kristensen, E.M. Bartels, H. Bliddal, A. Astrup, Lancet 370 (2007) 1706–1713.
[9] D.R. Janero, A. Makriyannis, Expert. Opin. Emerg. Drugs 14 (2009) 43–65.
[10] D. Jones, Nat. Rev. Drug. Discov. 7 (2008) 961–962.
[11] G.G. Muccioli, D.M. Lambert, Curr. Med. Chem. 12 (2005) 1361–1394.
[12] J.H. Lange, C.G. Kruse, Drug. Discov. Today 10 (2005) 693–702.
[13] J. Adam, P.M. Cowley, T. Kiyoi, A.J. Morrison, C.J. Mort, Prog. Med. Chem. 44 (2006) 207–329.
[14] B.E. Evans, K.E. Rittle, M.G. Bock, R.M. DiPardo, R.M. Freidinger, W.L. Whitter, G.F. Lundell, D.F. Veber, P.S. Anderson, R.S. Chang, et al., J. Med. Chem. 31 (1988) 2235–2246.
[15] A.A. Patchett, R.P. Nargund, Annu. Rep. Med. Chem. 35 (2000) 289–298.
[16] G. Muller, Drug. Discov. Today 8 (2003) 681–691.
[17] D.A. Horton, G.T. Bourne, M.L. Smythe, Chem. Rev. 103 (2003) 893–930.
[18] C.T. King, S.A. Weaver, J.E. Derr, Am. J. Obstet. Gynecol. 93 (1965) 563–565.
[19] R.A. Neal, J. Halpert, Annu. Rev. Pharmacol. Toxicol. 22 (1982) 321–339.
[20] K.S. Song, S.H. Lee, H.J. Chun, J.Y. Kim, M.E. Jung, K. Ahn, S.U. Kim, J. Kim, J. Lee, Bioorg. Med. Chem. 16 (2008) 4035–4051.